Available online at www.sciencedirect.com
SCIENCE DIRECT
Polymer 47 (2006) 672–678
polymer
www.elsevier.com/locate/polymer

# Preparation of natural rubber–montmorillonite nanocomposite in aqueous medium: evidence for polymer–platelet adhesion

L.F. Valadares, C.A.P. Leite, F. Galembeck *

*Institute of Chemistry, Universidade Estadual de Campinas, P.O. Box 6154, 13083-970 Campinas, SP, Brazil*

Received 15 July 2005; received in revised form 19 November 2005; accepted 21 November 2005
Available online 9 December 2005

**Abstract**

Nanocomposites of natural rubber latex and layered silicates are prepared by a mild dispersion shear blending process. The results of X-ray diffraction (XRD) and transmission electron microscopy (TEM) show that clay particles are well dispersed in the dry latex and the platelets have a preferential orientation, forming translucent nanocomposites. These show tensile mechanical properties analogous to those obtained with vulcanized rubber as well as an increased solvent resistance, which is expected considering that there is significant adhesion between clay lamellae and rubber. Nanocomposite swelling is strongly anisotropic. Natural rubber properties may thus be strongly modified by nanocomposite formation producing unprecedented combinations of properties.


*Keywords:* Nanocomposite mechanical properties; Anisotropic swelling; Rubber–clay platelet adhesion

## 1. Introduction

Polymer–clay nanocomposites have attracted the attention of many researchers and experimental results are presented in a large number of recent papers and patents because of the outstanding mechanical properties and low gas permeabilities that are achieved in many cases.

The advantages of nanocomposites containing single silicate layers uniformly dispersed in a polymer matrix were first demonstrated by researchers at Toyota in Japan who made a nylon-6 nanocomposite [1,2]. The procedure used the intercalative ring opening polymerization of ε-caprolactam within montmorillonite treated with ω-aminoacids, leading to the formation of exfoliated nanocomposites and showing a dramatic increase in Young modulus and tensile strength even at low filler content. Most important, the large increase in strength and modulus was not accompanied by a decrease in impact resistance that is usually the case with polymers filled with silica, calcium carbonate and other inorganic particles. Moreover, differences in the extent of exfoliation were also observed and these were shown to strongly influence the Young modulus, showing that particle dispersion down to the individual lamella level is actually desired to achieve maximum effect of nanocomposite formation [3].

Giannelis [4] showed that it is possible to melt-mix polymers with layered silicates using industrial processes like extrusion and/or mold injection. Using e.g. poly(ethylene oxide) with $Na^+$-montmorillonite (NaMMT) or polystyrene with organosilicate it is possible to obtain clay–polymer nanocomposites. Today, efforts are being conducted globally, using almost every type of polymer matrix [5].

The development of polymer–clay nanocomposites has been creating a number of technologies and opportunities that can be applied to natural rubber (NR). NR nanocomposites have been prepared using procedures derived from those used for thermoplastics, based on mixing solid rubber with organoclays. Arroyo et al. [6] studied the possibility of substituting carbon black by white fillers, e.g. a montmorillonite modified with octadecylamine. The organoclay behaves as an effective reinforcing agent of vulcanized rubber, showing a stronger reinforcing effect than carbon black while retaining the elasticity of the elastomer. This is opposed to the low reinforcement effect observed by the same authors, while using unmodified montmorillonite.

The solution method is also widely used to prepare nanocomposites [7,8] and it can be used with NR but this is very inconvenient due to the use of organic solvents.

During early work in this laboratory [9], it was realized that it should be possible to make nanocomposites with hydrophilic clays such as NaMMT but dispensing with the usual clay

* Corresponding author. Tel./fax: +55 19 37 88 30 80.
*E-mail address:* fernagal@iqm.unicamp.br (F. Galembeck).

0032-3861/$ - see front matter © 2005 Elsevier Ltd. All rights reserved.
doi:10.1016/j.polymer.2005.11.062

organophilic modification. Another relevant precedent to the present work is the discovery of a complex structure of nanodomains carrying excess electric charges in NR as well as synthetic latexes, pointing towards the contribution of electrostatic interactions to rubber cohesion and interfacial compatibility in single-phase and multiphase systems [10–12]. Considering that the latexes are aqueous polymer dispersions and water is an excellent exfoliating agent for clays [13], this led to work exploiting procedures based on mixing clay and latex within an aqueous dispersion.

Karger-Kocsis et al. [14–16] showed that the organophilic modification of the clay is not always necessary. They prepared nanocomposites drying a clay–NR latex dispersion and vulcanizating the rubber. Using this method with natural sodium bentonite and synthetic sodium fluorohectorite, vulcanized NR nanocomposites were obtained with great increase in modulus and tensile strength, especially in the case of fluorohectorite.

Besides the Karger-Kocsis study, there are few reports in the current literature on nanocomposites made by wet processing: Yu et al. prepared elastomeric nanocomposites based on the latex coagulation in acid media, using this technique for styrene–butadiene rubber [17–19] and carboxylated acrylonitrile–butadiene rubber [20]. These materials show better mechanical properties than those produced by the solution method described in the same paper [17]. InMat and Michelin [21] hold a patent that describes nanocomposite coatings preparation using elastomeric latexes.

However, the current literature does not describe the properties of bulk non-vulcanized NR nanocomposites. This paper shows a procedure to prepare these materials together with their properties, giving special attention to the clay–rubber interface.

## 2. Experimental section

### 2.1. Materials

Centrifuged NR latex with 61.7% dry rubber content (stabilized with 0.69% ammonia) was supplied by Riobor (São José do Rio Preto, SP) and it is a mixture extracted of RRIM 600, PB 235, GT-I, IAN 873 and PR 255 clones that are prevalent in the São Paulo state plantations. The clay used in this work is the NaMMT acquired from Southern Clay Products (cation exchange capacity = 92 mequiv./100 g of clay).

### 2.2. Synthesis of the nanocomposites

The amounts of water, latex and clay used in the preparation of the compound batches are given in Table 1 (phr = parts by weight, per 100 parts of rubber). The NaMMT was previously dispersed in water with continuous stirring using a Turrax mixer for 1 min at 13,500 rpm. The NR latex was added to the clay dispersion and stirred for 1 min at 24,000 rpm. The samples were then concentrated in a spinning evaporator (Rotavapor type) to remove water (Table 1) under reduced pressure. This produced thick slurries that were cast on flat plastic molds ($20\times10\times1.2$ cm$^3$, for the tensile tests and $70\times40\times2$ mm$^3$, for other measurements), using as many batches as required to fill the molds. The samples were dried in an oven under air at either 50 or 70 °C, as indicated in Table 1. Separate experiments (not shown) evidenced that drying temperature is not a relevant parameter, within this range.

### 2.3. Characterization of the nanocomposites

X-ray diffraction (XRD) measurements were performed in a Shimadzu XRD-6000 diffractometer using the reflection mode at a scan rate of 0.5°/min with Cu $K_\alpha$ X-ray radiation (= 1.54 Å) on the nanocomposite samples and on the film formed by drying an aqueous clay dispersion (1:100) (stratified clay).

Ultra thin (ca. 60 nm) sections for transmission electron microscopy (TEM) analysis were cut normal to the nanocomposite film plane, with a diamond knife at −110 °C using a Reichert Ultracut ultramicrotome cooled with liquid $N_2$.

Samples prepared by drying a drop of dilute dispersion of clay and latex over a microscope grid were analyzed using transmission electron microscopy associated to electron spectroscopy imaging (ESI-TEM). A Carl Zeiss CEM 902 (80 kV) transmission electron microscope fitted with a Castaing-Henry energy filter spectrometer was used. When the electron beam passes through the sample, interaction with different elements results in characteristic energy losses. The spectrometer separates electrons according to their energies and the microscope uses inelastic scattered electrons to form element-specific images. Characteristic energy losses from interaction of electrons with C (303 eV) and Si (132 eV) were selected with an energy slit of 20 eV. A detailed description of the phenomena involved is in Ref. [22]. The images were recorded using a Proscan high-speed slow-scan CCD camera and digitized (1024–1024 pixels, 8 bits) using the AnalySis software.

Specimens for tensile testing performed following DIN 52504 were cut from the samples prepared by casting.

Table 1
Amounts of components used in nanocomposite preparation

| Sample clay content (phr) | Water (g) | NR latex (g) | NaMMT (g) | Water removed in the spinning evaporator (g) | Drying temperature (°C) |
|---|---|---|---|---|---|
| 5 | 374.69 | 121.56 | 3.75 | 50 | 50 |
| 10 | 435.48 | 60.78 | 3.75 | 100 | 70 |
| 20 | 465.86 | 30.39 | 3.75 | 200 | 70 |
| 30 | 475.99 | 20.26 | 3.75 | 300 | 70 |

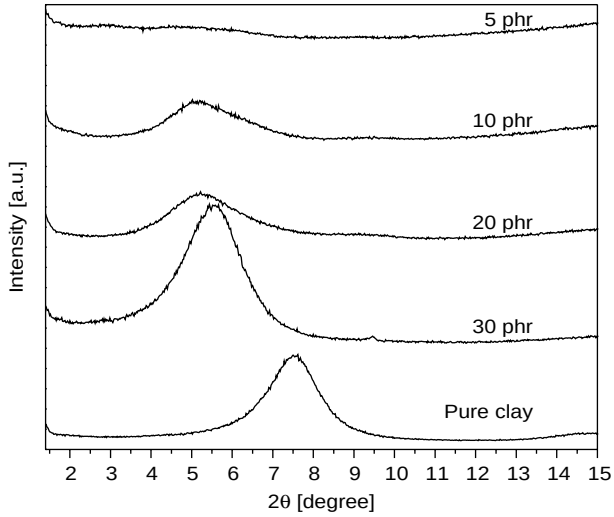


Fig. 1. XRD patterns for the pure clay and nanocomposites.

All specimens were kept at 23 °C in a 50% relative humidity for 24 h before the measurements were performed at room temperature, using an EMIC DL2000 universal testing machine at a strain rate of 200 mm/min. Five specimens were tested for each sample and the reported values are averages. The Young modulus [23] is obtained from angular coefficient in the initial linear portion ($\varepsilon < 0.5\%$) of the stress–strain plots.

For the swelling measurements, square specimens (1 cm wide, $\cong$0.5 mm thick) were cut and the thickness of each sample was measured using a micrometer. The initial weight was determined and the samples were immersed in xylene, within closed glass vials. They were periodically removed from the flasks, the adhering solvent was blotted off the surface and the samples were quickly weighed in an analytical balance. The lateral dimensions were also measured and the samples were immediately replaced in the flasks.

## 3. Results

XRD profiles in the 1.4–15° range of the pristine clay and nanocomposites are present in Fig. 1. The NaMMT shows a (001) diffraction peak at $2\theta = 7.52°$, which is assigned to the basal spacing of 1.17 nm but the composites do not show this peak. The 30 phr sample diffractogram shows an inter-lamellar distance ($d_{(001)}$) equal to 1.59 nm, the 20 phr shows $d_{(001)} =$ 1.69 and 1.72 nm in the 10 phr, while the 5 phr composite shows a low-angle broad halo. The broadening of the (001) peak in a low-angle region indicates the extensive layer separation associated to the clay lamellae intercalation and exfoliation. Assuming a full separation of single lamellae,

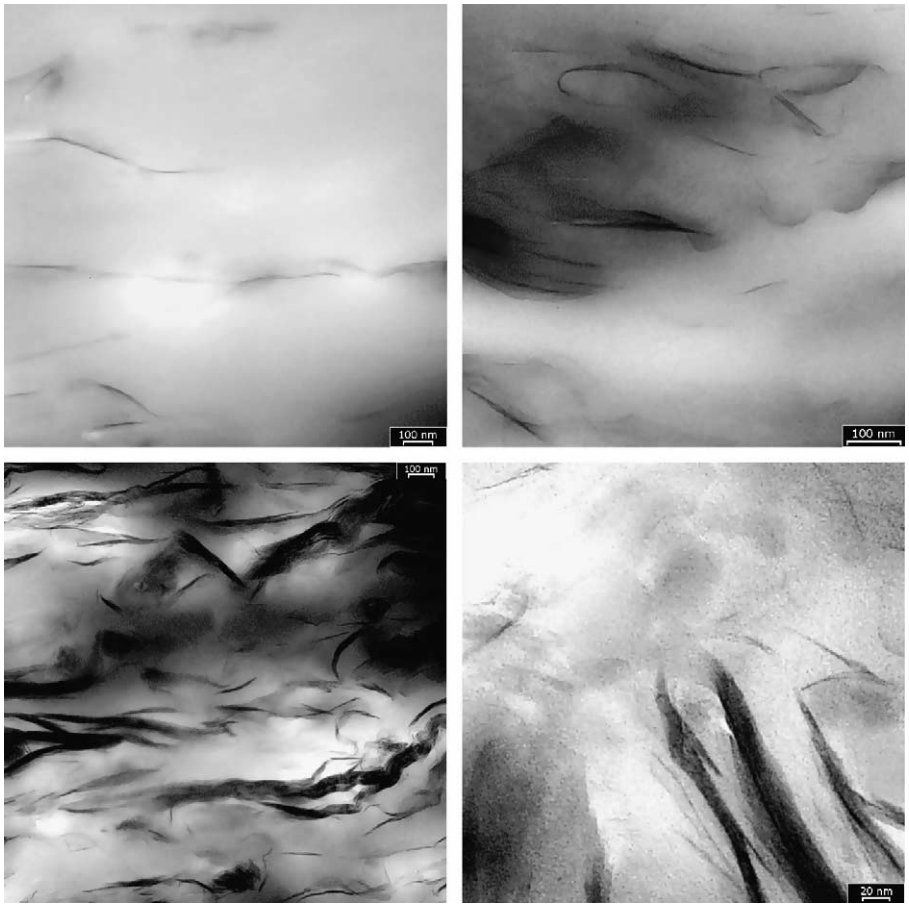


Fig. 2. TEM micrographs of 5 phr (a top) and 30 phr (bottom) NaMMT–NR composite. The thin cuts were made normal to the nanocomposite film plane.

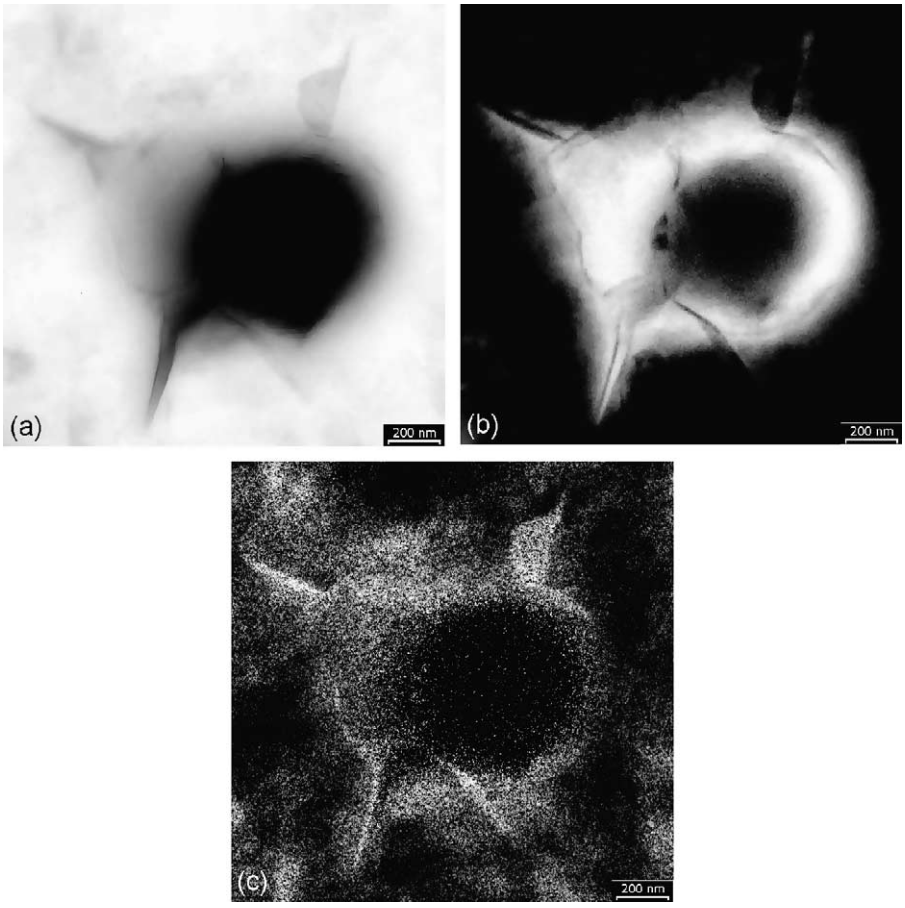


Fig. 3. ESI-TEM micrographs of a rubber–clay particles cluster formed when a dilute dispersion of latex and montmorillonite is allowed to dry over a microscope grid: (a) bright field image, (b) carbon map and (c) silicon map.

average interparticle distances should be ca. 61 nm for the 5 phr sample and 11 nm for the 30 phr sample. This means that the peaks observed in the X-ray diffractograms are due to rubber intercalation within lamellae stacks or tactoids.

TEM micrographs of thin cuts of dry nanocomposites are given in Fig. 2. The dark lines are the cross-sections of single or multiple silicate platelets. These are flexible and they often appear curved. Their thickness is in the 3 nm range in the micrographs of the 5 phr sample while the observed average length is ca. 130 nm. The thickness observed from these micrographs is higher than that of a single MMT layer, which is about 1 nm. This was also observed by Cho and Paul [24] and the possible reasons are as follows. First, the MMT platelets are not completely exfoliated and a significant number of two-, three- or four-lamellae tactoids is actually seen. Second, the microtoming direction may not be perfectly normal to the surface of the platelets and therefore the image shows tilted platelets that appear thicker. Finally, there is always the possibility of imperfect focusing of these unstable samples, in the TEM.

The 5 phr samples images confirm the X-ray data, showing that the clay is well exfoliated in the NR matrix and the individual layers are coarsely aligned along the nanocomposite dry film plane.

In the 30 phr sample, TEM images show mainly tactoids but it is also possible to observe exfoliated structures with single 1 nm thick platelets. Most important, void formation in the polymer–filler interface is never observed, providing a strong evidence for good adhesion between the clay lamellae and the rubber.

ESI-TEM micrographs were also taken from very dilute clay–rubber latex dispersions that were allowed to dry on carbon films over the microscope holder grids, shown in Fig. 3. The three images in Fig. 3 correspond to the same field. The bright field image (Fig. 3(a)) provide a fine contrast allowing the observation of a detailed morphology. The carbon (Fig. 3(b)) and silicon (Fig. 3(c)) maps are very useful to identify the location of the rubber and the clay particles, respectively. The darkness of the rounded area near the center of the cluster, that appears in all images, is due to excessive thickness.

Fig. 3 shows a rubber particle, approximately spherical, in the center of the image. There are some clay particles without contact with the rubber lying in the image plane and these produce low contrast in the bright field image because they are very thin. Many other clay particles are in contact with the rubber and these are oriented normal to the image plane. These particles produce high contrast due to their alignment that produces strong interaction with the electron beam.

The superimposition of clay and rubber domains (as opposed to mutual exclusion) and the deformation of rubber and clay particles is a strong evidence in favour of clay–rubber

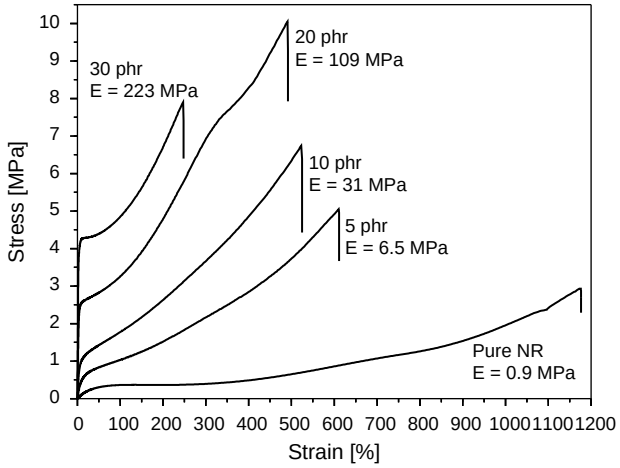


Fig. 4. Stress vs. strain curves for NR and NaMMT filled composites.

compatibility, that is all but unexpected due to the great differences between the properties of the two phases.

Stress vs. strain curves are in Fig. 4, showing that the nanocomposites present initial moduli and tensile strengths greater than NR. The Young modulus increases with the clay content, as much as 250-fold. The tensile strength of the composites shows a maximum between 20 and 30 phr, what is an unusual behavior. An interesting feature is the shape of the stress vs. strain curve for the composites: the high moduli, tensile strength, tenacity and the presence of a yield point in this curve do not resemble known behavior for vulcanized rubber but they are rather similar to that observed for semi-crystalline thermoplastics.

We can conclude that the increase of clay content in the NR matrix causes a drastic influence in the mechanical properties of the composite, increasing the Young moduli and tensile strength of materials, but partially preserving the characteristic rubber elongation and thus resulting in tenacious materials.

Swelling behavior was observed by determination of xylene sorption as a function of time. Xylene mass uptake is significantly decreased in the 30 phr but not in the 5 phr nanocomposite, as compared to NR (shown in Fig. 5). Moreover, the 30 phr nanocomposite sample can still be easily handled 2 h after immersion in xylene, keeping its physical integrity while the NR samples tear very easily upon handling in less than 1 h, under the same conditions.

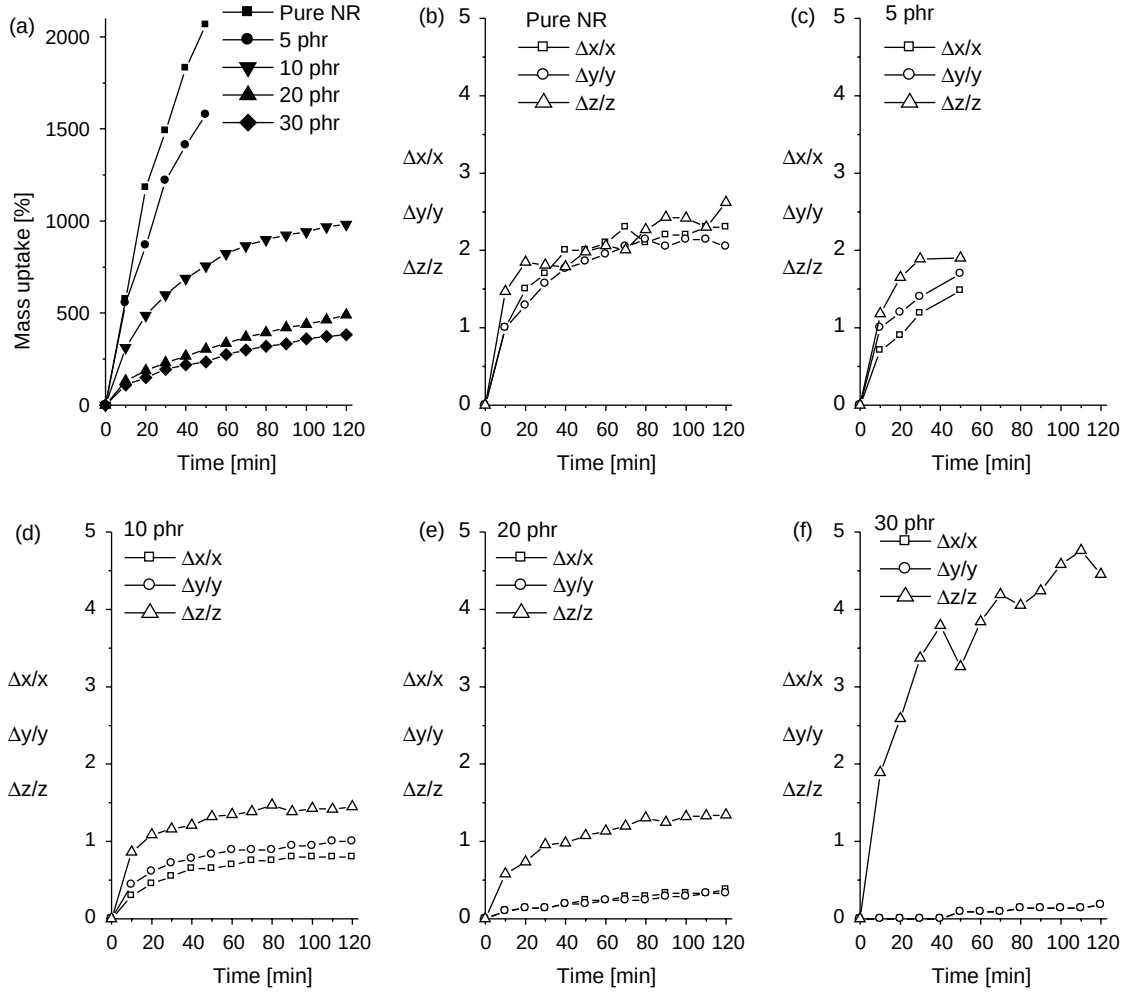


Fig. 5. Xylene sorption in NR and NaMMT–NR composites. (a) Mass uptake. The other plots are dimension changes in (b) pure rubber, (c) NR + 5 phr MMT, (d) NR + 10 phr MMT, (e) NR + 20 phr MMT and (f) NR + 30 phr MMT. The *x* and *y* lengths are along the film plane.

Measuring the changes in the lateral ($x$–$y$) dimensions of thick film samples and calculating the change in thickness ($z$) by using the mass uptake in the swelling experiments, it is possible to observe a strong swelling anisotropy in the 20 and 30 phr samples: the film $x$–$y$ coordinates (in the film plane) change much less than the $z$ coordinate (normal to the plane of the film), as shown in Fig. 5.

## 4. Discussion

The results presented in this paper show that NR–clay nanocomposites are obtained using rubber latex and hydrophilic clay following a mix-and-dry procedure that is both convenient and effective. A first question is, why does this procedure work? Some answers may be offered to this question: first, water is an excellent exfoliating agent for montmorillonite clay [13] and both clay and rubber particles carry excess of negative charges, thus they form stable dispersions. Upon drying, the clay and rubber particles undergo capillary adhesion that is sufficiently strong to produce the rubber particle–clay platelet clusters clearly shown in the micrographs in Fig. 3. After drying, counter-ions are clustered in between rubber and clay particles thus making an electrostatic contribution to cohesion in this system.

Demixing between clay and rubber is expected on thermodynamic grounds but it is countered by adhesion as described in the previous paragraph and it is also kinetically limited by the slow diffusion of the clay platelets and rubber chains so that the intercalated or exfoliated patterns persist and they can be observed in the dry nanocomposites.

The mechanical behavior of the 20–30 phr nanocomposites is akin to that of a semi-crystalline thermoplastic like LDPE or MDPE, considering the initial modulus, the significant flow at higher stresses and even the tensile strength, see Table 2.

The anisotropic swelling behavior of the non-vulcanized nanocomposites is analogous to the observed by Karger-Kocsis et al. for vulcanized natural rubber [14]. Considering that solvent diffusion in the nanocomposite is impaired by the clay platelets and that these do not absorb solvent, a decrease in the nanocomposite swelling rate and swelling coefficient is expected, as the clay content increases. However, the swelling anisotropy can only be understood considering that the platelets are roughly parallel to the film plane (as seen in the TEM micrographs) and that there is significant clay–rubber adhesion, sufficient to limit rubber chain extension in the film plane in the presence of the solvent. On the other hand, the inter-platelet space is filled with rubber chain segments that are not directly bound to the clay platelets and these are thus freer to expand as the solvent is absorbed. Moreover, clay platelets are self-aligned upon composite dispersion drying and this may be assigned to the minimization of overall electrostatic energy in this system as well as to hydrodynamic factors. However, these are only hypotheses that will be tested in future work. This unique behavior opens a number of possibilities that could be exploited in the near future and an attractive possibility is the verification of a strong anisotropy of diffusion coefficients and other transport-related properties, in the nanocomposite films.

Table 2
Mechanical properties of nanocomposites compared to typical values for rubbers and plastics [25]

| Material | Young modulus (MPa) | Max strain (%) | Tensile strength (MPa) |
|---|---|---|---|
| Pure gum vulcanized | 1.3 | 750–850 | 17–25 |
| Vulcanized NR 33% carbon black | 3–8 | 550–650 | 25–35 |
| LDPE | 55.1–172 | 150–600 | 15.2–78.6 |
| MDPE | 172–379 | 100–150 | 12.4–19.3 |
| HDPE | 413–1034 | 12–700 | 17.9–33.1 |
| Unvulcanized NR[a] | 0.9 | 1150 | 3 |
| 5 phr-Nanocomposite[a] | 6.5 | 599 | 4.9 |
| 10 phr-Nanocomposite[a] | 31 | 496 | 6.5 |
| 20 phr-Nanocomposite[a] | 109 | 460 | 9.7 |
| 30 phr-Nanocomposite[a] | 223 | 245 | 7.9 |

[a] This work.

Together, the present results show that rubber intercalation within the clay lamellae also makes an important contribution to the composite properties, adding up to the exfoliated clay. Indeed, both types of dispersed lamellae can make different but synergistic contributions to nanocomposite properties.

## 5. Conclusion

Unvulcanized natural rubber nanocomposites with interesting mechanical properties are prepared by a simple procedure using aqueous dispersion. Clay platelets are oriented within the cast films and there is strong adhesion at the rubber–clay interface, assigned to electrostatic interaction between clay, rubber and the dry serum counter-ions. This adhesion creates the possibility to prepare nanocomposites with highly variable mechanical properties just by changing the clay content.

## Acknowledgements

L.F.V. acknowledges a fellowship from CAPES. This is a contribution from the Millenium Institute for Complex Materials, PADCT/CNPq. The authors thank Riobor for the NR latex.

## References

[1] Usuki A, Kojima Y, Kawasumi M, Okada A, Fukushima Y, Kurauchi T, et al. J Mater Res 1993;8(5):1179–84.
[2] Kojima Y, Usuki A, Kawasumi M, Okada A, Fukushima Y, Kurauchi T, et al. J Mater Res 1993;8(5):1185–9.
[3] Kojima Y, Usuki A, Kawasumi M, Okada A, Kurauchi T, Kamigaito O. J Polym Sci, Part A: Polym Chem 1993;31(7):1755–8.
[4] Giannelis EP. Adv Mater 1996;8(1):29–35.
[5] Ray SS, Okamoto M. Progr Polym Sci 2003;28(11):1539–641.
[6] Arroyo M, López-Manchado MA, Herrero B. Polymer 2003;44(8):2447–53.
[7] Vu YT, Mark JE, Pham LH, Engelhardt M. J Appl Polym Sci 2001;82(6):1391–403.
[8] Joly S, Garnaud G, Ollitrault R, Bokobza L, Mark JE. Chem Mater 2002;14(10):4202–8.

[9] Galembeck F, Souza MDFB. WO Patent 2005030850; 2005.
[10] Rippel MM, Leite CAP, Galembeck F. Anal Chem 2002;74(11):2541–6.
[11] Santos JP, Corpart P, Wong K, Galembeck F. Langmuir 2004;20(24): 10576–82.
[12] Braga M, Costa CAR, Leite CAP, Galembeck F. J Phys Chem B 2001; 105(15):3005–11.
[13] Norrish K. Discuss Faraday Soc 1954;18:120–34.
[14] Varghese S, Karger-Kocsis J. Polymer 2003;44(17):4921–7.
[15] Karger-Kocsis J, Wu CM. Polym Eng Sci 2004;44(6):1083–93.
[16] Varghese S, Karger-Kocsis J. J Appl Polym Sci 2004;92(1):543–51.
[17] Wang Y, Zhang L, Tang C, Yu D. J Appl Polym Sci 2000;78(11):1879–83.
[18] Zhang L, Wang Y, Wang Y, Sui Y, Yu D. J Appl Polym Sci 2000;78(11): 1873–8.
[19] Wu YP, Wang YQ, Zhang HF, Wang YZ, Yu DS, Zhang LQ, et al. Compos Sci Technol 2005;65(7–8):1195–202.
[20] Wu Y, Zhang L, Wang Y, Liang Y, Yu D. J Appl Polym Sci 2001;82(11): 2842–8.
[21] Feeney CA, Farrell M, Tannert K, Goldberg HA, Lu M, Grah MD, Steiner, WG, Winston PB. US Patent 6 232 389; 2000.
[22] Keslarek AJ, Leite CAP, Galembeck F. J Braz Chem Soc 2004;15(1): 66–74.
[23] Hunt BJ, James MI. Polymer characterisation. London: Chapman and Hall; 1997 p. 362.
[24] Cho JW, Paul DR. Polymer 2001;42(3):1083–94.
[25] Brandup J, Immergut EH. Polymer handbook. New York: Willey; 1975 [chapter V].